International Journal of Pharmaceutics, 39 (1987) 213–227
Elsevier

IJP 01329

Localization of colloidal particles (liposomes, hexylcyanoacrylate nanoparticles and albumin nanoparticles) by histology and autoradiography in mice

P.G. Waser [1], U. Müller [1], J. Kreuter [2], S. Berger [1], K. Munz [1], E. Kaiser [1] and B. Pfluger [1]

[1] *Institute of Pharmacology, University of Zürich (Switzerland) and* [2] *Institute of Pharmaceutical Technology, J.W. Goethe-University, Frankfurt / Main (F.R.G.)*

(Received 8 April 1987)
(Accepted 15 May 1987)

Key words: Albumin nanoparticle; Polyalkylcyanoacrylate nanoparticle; Diazepam; Liposome; Autoradiography on macro-, micro- and electron microscopic level; Tissue distribution; Tissue interaction

Summary

Distribution and uptake of 3 labeled colloidal carrier systems have been studied following i.v. injection in mice: [^{14}C]diazepam liposomes, [^{14}C]polyhexylcyanoacrylate nanoparticles and ^{125}I-albumin nanoparticles. All systems accumulated in the organs of the reticuloendothelial system (RES). Targeting to a specific organ was not achieved. Concentration kinetics revealed that [^{14}C]diazepam was eliminated together with the lipids without any redistribution of the drug in the body. After 10 days, only radioactivity of the nanoparticle systems remained on a relatively high level in the organs of the RES. Whole-body and light microscopic autoradiographs of [^{14}C]polyhexylcyanoacrylate and ^{125}I-albumin nanoparticles revealed an unusual spotted appearance of silver grains in liver, lungs and bone marrow. Ultrastructural investigations of liver and lung tissue demonstrated incorporation of polyhexylcyanoacrylate nanoparticles into hepatocytes and pulmonary cells 5 min after injection and possibly microembolism for albumin and cyanoacrylate nanoparticles.

Introduction

During the two past decades drug carrier systems have been investigated in order to achieve targeting of drugs in specific organs and sustained release of the active principles. The injection of particles with adsorbed active substances has been suggested to improve efficacy and reduction of untoward side effects. It has been shown that particle size, surface properties of matrix material and route of administration are of importance. Various contributors describe the physical, chemical, biological, pharmacokinetic and therapeutic aspects of such systems (Gregoriadis, 1979; Juliano, 1980).

The present investigation compares the distribution pattern of 3 different carrier systems with respect to precise localization of the carrier material in the body and integrity of the target tissue. A unilamellar liposome system (ULL) (Müller et al., 1983) and two colloidal nanoparticle systems consisting of polyhexylcyanoacrylate (PHCA) (Couvreur et al., 1979; Lenaerts et al., 1982; Gipps et al., 1986) respectively of serum

Correspondence: U. Müller, Institute of Pharmacology, University of Zürich, Gloriastrasse 32, CH-8006 Zürich, Switzerland.

albumin (albumin) (Scheffel et al., 1972; Widder et al., 1979; Gallo et al., 1984) were applied. Our studies also investigate the fate of colloidal particles and their long term persistence (10 days) in several organs after intravenous injection in mice. Colloidal particles are known to be distributed largely as a function of their size and their surface properties (Kreuter, 1983a; Leu et al., 1984). Large particles (> 7 μm) are mostly trapped mechanically in the pulmonary vessels (Kanke et al., 1980; Slack et al., 1981), whereas small particles (< 1000 nm) are taken up preferentially by the cells of the reticuloendothelial systems (RES). The phagocytotic process is rapid and efficient: 5 min after i.v. injection 90% of the particles are removed from the blood stream being localized in the liver, lungs, spleen and also in the bone marrow (Grislain et al., 1983). The first part of our study was carried out using the technique of whole body autoradiography. The second part includes histology and autoradiography of lungs and liver tissue by light and electron microscopic techniques.

Materials and Methods

Preparation of [^{14}C]diazepam-phospholipid vesicles (liposomes)

10 mg phosphatidylcholine (egg lecithin) and 1.8 mg of phosphatidic acid (20 mol%) were dissolved in 30 ml of chloroform/methanol (1 : 1, v/v) in a 100-ml round flask. The solvent was then removed under reduced pressure on a rotary evaporation apparatus leaving a thin film on the glass wall. Thereafter, 4.5 mg of [^{14}C]diazepam (67 μCi) in 1.3 ml of 0.3 M PIPES buffer (pH 7.2) which contained 30 mM sodium cholate was added. Brief mechanical shaking allowed the lipid–drug–detergent mixture to form a dispersion which was left for 30 min at room temperature for equilibration. This dispersion was centrifuged through a Sephadex G-50 column adapted into a GSA rotor of a Sorvall centrifuge. The Sephadex was equilibrated too for 30 min at 4 °C with 12 ml of the above buffer and the void volume separated by centrifugation at 1000 *g* for 10 min. The final volume of 1.23 ml had an activity of 36 μCi (48% of the initial activity). The particle size of the liposomes as determined by transmission electron microscopy after negative staining was between 50 and 70 nm.

Preparation of [^{14}C]polyhexylcyanoacrylate nanoparticles

Hexyl-[3-^{14}C]cyanoacrylate was dispersed by means of mechanical stirring at 4 °C in 100 ml of an aqueous solution containing 50% 0.1 M HCl, 0.2% w/v Pluronic F 68 and 1% w/v dextran 70. After 4 days, polymerization was complete and the pH was adjusted to 7.0 with 1 M NaOH. The resultant suspension was lyophilized and the powder was stored at 4 °C. Before injection, the lyophilizate was resuspended in water containing 0.5% Pluronic F 68 by ultrasonication. The final concentration of polymer was 6 mg/ml, equivalent to about 10^{12} nanoparticles/ml with a radioactivity of 4.5 μCi/ml. The nanoparticle preparation thus produced was examined by transmission electron microscopy using negative staining by phosphotungstic acid. Non-aggregated nanoparticles with sizes varying between 200 and 300 nm were observed.

Preparation of ^{125}I-albumin particles

125 mg of ^{125}I-bovine serum albumin (0.5 mCi) were dissolved in 0.5 ml deionized distilled water. This aqueous solution was combined with 30 ml of soya oil at 4 °C and ultrasonicated for 10 min at 60 W power setting prior to addition of portions of 6 ml of this emulsion to 100 ml soya oil. Each portion of the emulsion was added dropwise (40 drops/min) to the soya oil at 140 °C ± 7 °C which was being stirred at 1500 rpm. After the emulsion was added, heating was continued for 10 min. The suspension was then allowed to cool to 25 °C. Once this temperature had been reached, stirring was stopped and 100 ml of anhydrous ether was added to the particle-soya oil suspension. The mixture was centrifuged at 3000 *g* for 15 min. The supernatant was decanted. 100 ml of anhydrous ether was again added to the nanoparticle pellet. The particle pellet was resuspended in the ether using an ultrasonic water bath. This suspension was then centrifuged at 3000 *g* for 15 min. This washing step was repeated twice. The final pellet was resuspended in 10 ml of anhydrous ether,

passed through a G1 glass sinter filter, and after evaporation of the ether, stored at 4°C in an air-tight container. The powder was resuspended in physiological saline containing 0.1% polysorbate 80 and sonicated for 10 min prior to injection. The size of individual particles ranged from 500 to 1300 nm with mean diameter around 750 nm as determined by transmission electron microscopy.

Determination of soluble radioactivity in [^{14}C]polyhexylcyanoacrylate nanoparticles

After resuspension of the lyophilized nanoparticles in water, an aliquot of 10 µl was transferred into a centrifugation tube, diluted with 1 N HCl to 100 µl. An aliquot of 10 µl of this dilution was counted in a liquid scintillation counter (Beckman LS 180/MU). After centrifugation at 100,000 × *g* for 15 h in an air-driven ultracentrifuge (Beckman Airfuge), 10 µl of the supernatant was also counted in the liquid scintillation counter. Over 99.88% of the radioactivity was associated with the centrifugation pellet.

Animal experiments and preparation of cryosections

Male albino mice, strain ICR with an average weight of 20 g, were used. Groups of 3 animals were injected with the labeled carrier materials into a tail vein, the injected radioactivity ranging from 44 to 210 nCi/g of animal weight. After appropriate time intervals, namely 2, 5 and 30 min, 2 and 6 h, respectively 10 days, the animals were killed with ether and submerged in a mixture of hexane/carbon dioxide (−78°C).

The frozen animals were then embedded in 5% sodium carboxymethylcellulose in a metal frame and immediately frozen at −78°C. Whole body sagittal sections were adhered to Scotch tape 3M 810 and freeze dried at −20°C for 48 h. Some sections were stained with hematoxylin-eosin.

Whole body autoradiography and quantitative determination of radioactivity in the organs

Sections were exposed to Kodak X-ray film DEF-5 at −20°C up to 14 weeks and the films were developed in Kodak D-19. Blackening of the film was measured using a transmission densitometer (Macbeth TD-504) and compared with standards, containing a scale of 16 dilution concentrations with [^{14}C]glucose, as described by Cross et al. (1974). The data of the ^{125}I-label experiments resulted from gamma counting (Nucletron CG 4000) of excised tissue samples.

Light microscopic autoradiography

Tissue samples from excised organs were rapidly frozen in viscous isopentane, transferred into liquid nitrogen and stored in a refrigerator at −70°C until further processing. Sections of 10 µm were cut with a Cryocut II Microtome (Reichert Jung) and mounted on slides covered with chrome alum-gelatine.

For autoradiography, Kodak fine grain stripping film AR-10 was used. The detailed method is given by Rogers (1979). After 5–9 days of exposure at −20°C, the films were developed with Kodak D 19 and stained with hematoxylin.

Electron microscopy

Cryofixation and freeze substitution

Fresh tissue from various organs of a mouse were cut into small pieces of about 1 mm^3, prefixed with 2.5% glutaraldehyde in Sörensen buffer pH 7.0 for 10 min and after addition of 30% glycerol as a cryoprotectant, rapidly frozen by dipping into liquid propane (−180°C). To avoid solubilization of the PHCA nanoparticles by the solvents routinely used for dehydrating and embedding procedures, the cryofixed samples were freeze substituted and embedded either in low temperature embedding medium Lowicryl K4M (Fluka, Buchs, Switzerland) according to Müller et al. (1980), or in Araldite/Epon mixture. Ultrathin sections were stained with uranyl acetate and lead citrate and observed in a Philips 400 T electron microscope.

Autoradiography

Ultrathin sections were placed on 200 mesh copper grids which had been coated with Collodium film and reinforced with carbon. 6–12 grids were then mounted onto glass slides with a touch of glue on two sides. These mounted grids were coated with Ilford L4 Nuclear Emulsion (Ilford Ltd., Ilford, U.K.) by the dipping method (dilution 1 : 2 with distilled water). Coated slides

were thoroughly air-dried and stored in the dark for 20 days in plastic boxes at −20 °C. Development of the autoradiographs was carried out according to standard methods. After prolonged washing in distilled water, the wet grids were immediately stained with lead citrate.

Results

Whole-body autoradiography

The distribution of radioactivity (RA) in the organs 5 min, 6 h and 10 days after i.v. injection of the 3 biodegradable particle systems is shown in Figs. 1–8.

Five min after i.v. injection

Fig. 1 shows the autoradiograph of [^{14}C]liposomes, respectively that of [^{14}C]diazepam incorporated in the lipid bilayer. The radioactivity reaches the brain only in a negligible quantity. In contrast, the appearance of RA in liver, kidney and intestine including gall bladder is surprisingly high at such an early time which is an indication for rapid elimination of the drug from the body. The adipose tissue of the neck and salivary gland and the mucosa of the pharynx and nose represent remarkable sites of incorporation of RA. Lungs and peripheral organs remain free of RA.

Fig. 2. In the case of PHCA nanoparticles, most of the RA is transported into the organs of the RES: lungs, liver, spleen and bone marrow. Again, remarkable quantities of RA appear in the blood vessels of the neck, heart, kidney and urinary system. In addition, considerable RA remains in the vena cava.

Fig. 3. After administration of ^{125}I-albumin nanoparticles, the RA is located primarily in the lungs. The rest of the RA is sited in small spots in liver, spleen and kidney (spleen is not visible in Fig. 3). The lung capillaries obviously act as filter for the albumin particles.

Six h after i.v. injection

Fig. 4. Administration of ULL leads to accumulation of RA in liver, intestine and kidney. Elimination of RA is continued and no redistribution of drug in the body liberated from the carrier material can be detected which is demonstrated by the fact that the brain contains only small amounts of [^{14}C]diazepam. In the adipose tissue of the neck, RA is diminished significantly.

Fig. 5. Accumulation of PHCA nanoparticle RA occurs specifically in the lungs and the liver and to a minor degree in the spleen and the bone marrow. Small spots of RA can be found in peripheral tissue.

Fig. 6. RA of injected ^{125}I-albumin particles is visible in a spotted form. Lungs and liver remain the main site of RA accumulation. In addition, at this time, RA is also found in the urinary system. Accumulation of RA in the thyroid gland is due to absorption of ^{125}I-label.

Ten days after i.v. injection

Fig. 7. After administration of PHCA nanoparticles, autoradiographs show a further concentration of RA in the RES. In the lungs, but also in the other organs of the RES, RA manifests itself in rough spots of concentrated silver grains indicating cluster formation. This accumulation of RA results from the small spots already observed at earlier times.

Fig. 8. After administration of ^{125}I-albumin nanoparticles, RA in the lungs and in the liver has diminished but is still visible as numerous small spots.

Kinetics

The quantitative distribution of the 3 labeled particle systems in the organs is compared in a kinetic analysis shown in Fig. 9. Only the organs with major accumulation of RA are presented. In the experiments with [^{14}C]diazepam containing liposomes, liver, kidney, bile and gastrointestinal tract accumulate RA in the first 30 min. RA in the liver decreases gradually within 6 h to 50% of the concentration found after 2 min. Only minor RA is observed in the brain decreasing continuously by 15% within 2 and 5 min and further by 37% between 5 min and 6 h. Almost no RA is detected in the lungs. No redistribution of released free diazepam by the blood can be observed as shown by lack of RA in the brain and other organs after 10 days. Elimination of this carrier system with the bile seems to be the main pathway.

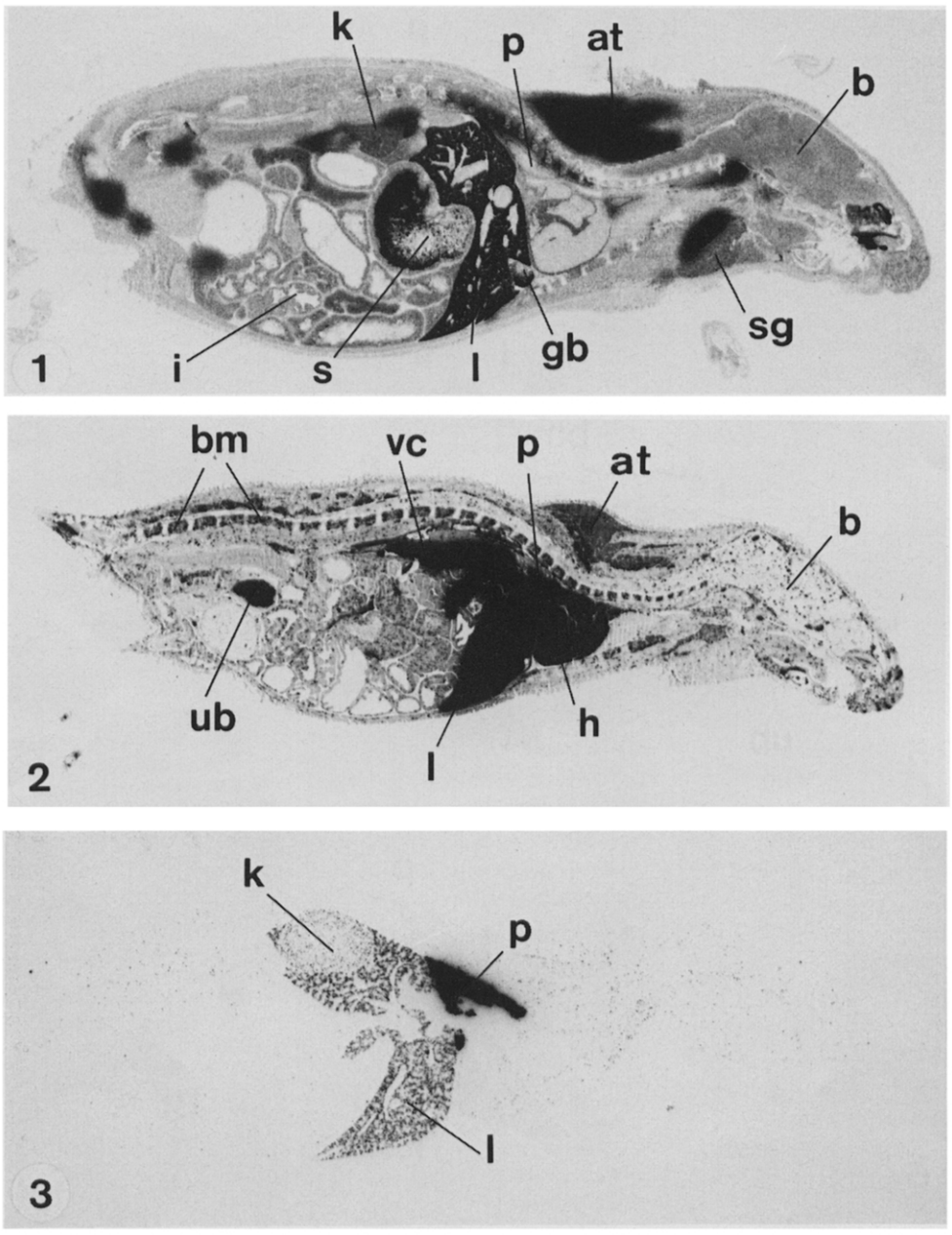

Figs. 1–3. Whole-body autoradiographs.

Fig. 1. Five min after i.v. injection of [^{14}C]diazepam liposomes. Most of the label (radioactivity) is found in the liver (l), stomach (s), adipose tissue (at) and kidney (k). Only little radioactivity is found in the lungs (p).

Fig. 2. Five min after i.v. injection of [^{14}C]polyhexylcyanoacrylate nanoparticles. Radioactivity is localized in liver (l), lungs (p) and bone marrow (bm). Radioactivity is also found in adipose tissue (at) and in the central vein (vc). Clusters of radioactivity are incorporated into the brain (b).

Fig. 3. Five min after i.v. injection of ^{125}I-albumin nanoparticles. Radioactivity is spottedly incorporated into lungs (p), kidney (k) and liver (l). h, heart; i, intestine; gb, gall bladder; sg, salivary gland; ub, urinary bladder.

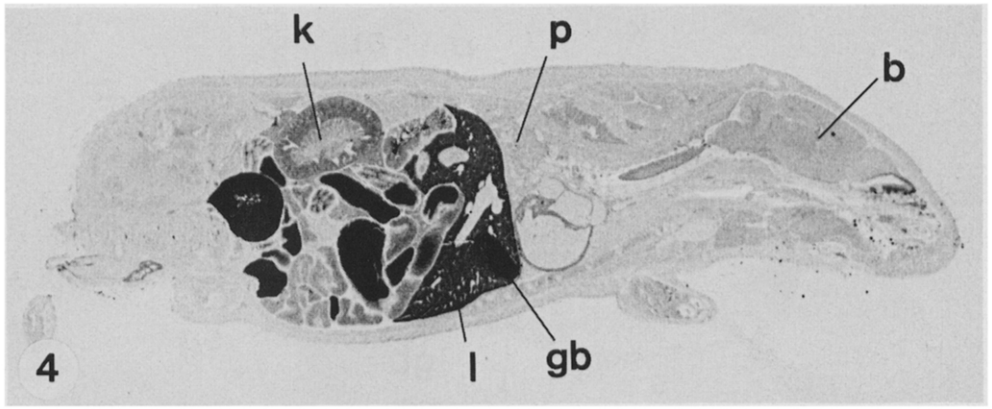

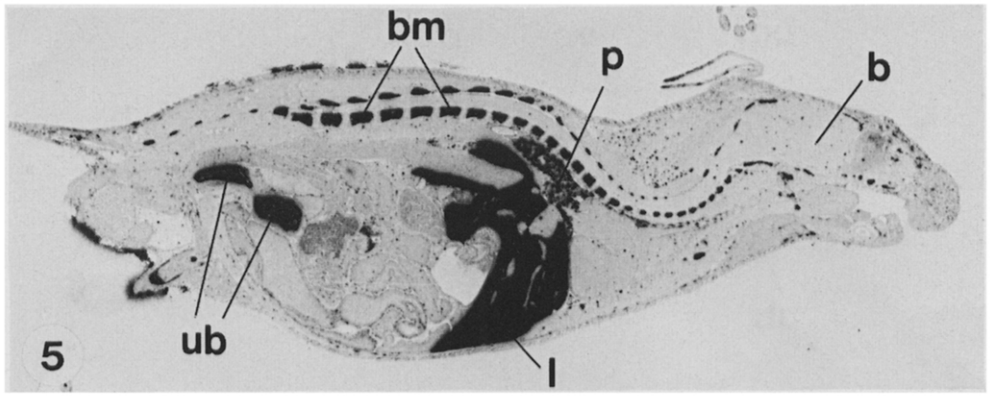

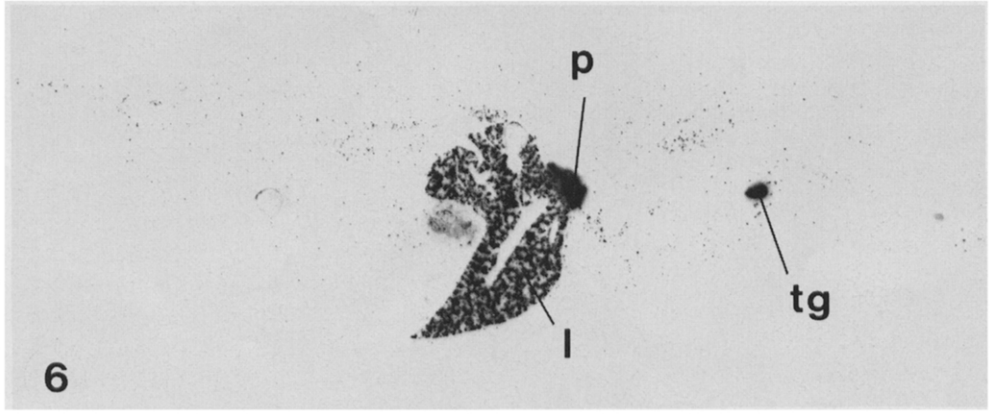

Figs. 4–6. Whole-body autoradiographs.

Fig. 4. Six h after i.v. injection of [^{14}C]diazepam liposomes. Label (radioactivity) is localized in liver (l), gall bladder (gb) and kidney (k). Little radioactivity is detected in lungs (p) and brain (b).

Fig. 5. Six h after i.v. injection of [^{14}C]polyhexylcyanoacrylate nanoparticles. Radioactivity is localized in liver (l), lungs (p), bone marrow (bm) and urinary bladder (ub). Minimal radioactivity is seen in the brain (b).

Fig. 6. Six h after i.v. injection of ^{125}I-albumin nanoparticles. Radioactivity is localized in lungs (p), liver (l) and typically in the thyroid gland (tg).

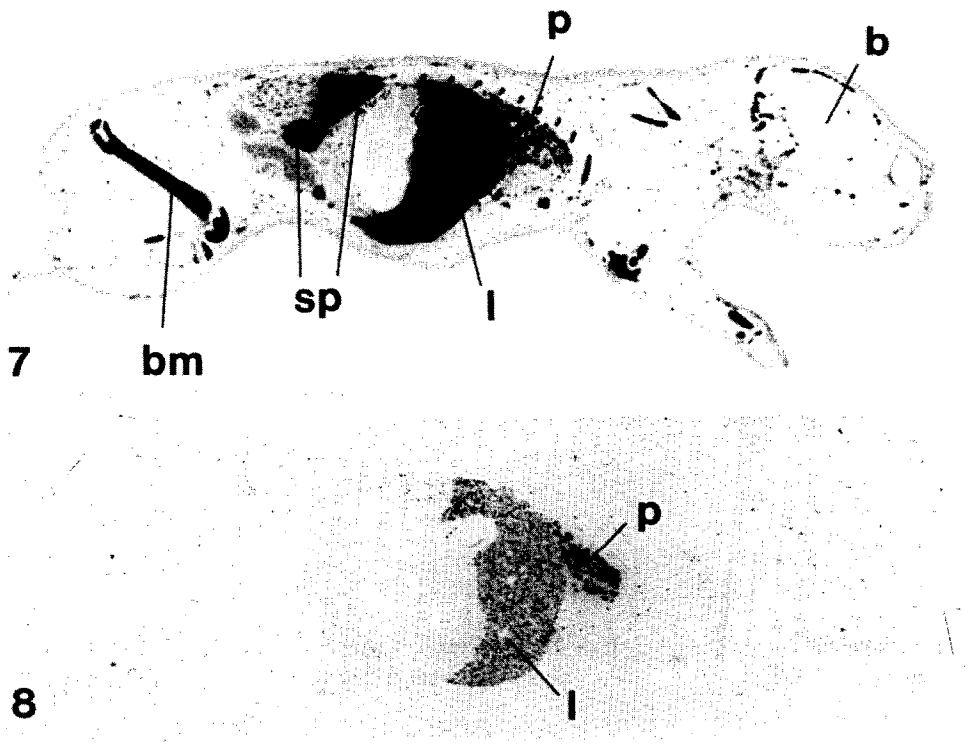

Figs. 7, 8. Whole-body autoradiographs.
Fig. 7. Ten days after i.v. injection of [^{14}C]polyhexylcyanoacrylate nanoparticles. Label (radioactivity) is still found in the organs of the RES: liver (l), lungs (p), spleen (sp) and bone marrow (bm). No radioactivity is detected in the brain (b).

Fig. 8. Ten days after i.v. injection of ^{125}I-albumin nanoparticles. Only minor quantities of radioactivity are detected in lungs (p) and liver (l).

Following the time course of PHCA particles, accumulation occurs to a high degree in the organs of the RES within the first minutes after i.v. injection into the animals. A high level of RA is observed in liver, spleen and bone marrow and to a lesser degree also in the lungs after 6 h. Most of the RA is found in the liver decreasing only slightly between 5 min and 6 h and by 4.5% between 6 h and 10 days. In contrast, RA accumulated in the lungs disappears faster, namely by 85% during the first 6 h and additional 4% in the following 10 days. The concentration in the spleen after 5 min is below 50% of that of the liver. After 6 h, there is an increase to 85% of the liver value and after 10 days, the remaining RA is still 80% of the liver activity. The same kinetic is found in the bone marrow, after 6 h, RA increases by a factor of 3 compared to the initial concentration and decreases again within the next 10 days by 50%. RA in the kidney decreases comparatively rapidly to an undetectable level within 10 days. The kinetics of ^{125}I-albumin particles (Fig. 9c) may be analysed as follows: main accumulation is occurring within 5 min in liver, lungs and spleen and a high level of RA remains in these organs up to 6 h. In contrast to the PHCA particles RA drops within 10 days to low levels in all organs. RA found in the kidney indicates the main elimination route from the body. No redistribution of albumin particles to peripheral organs was observed.

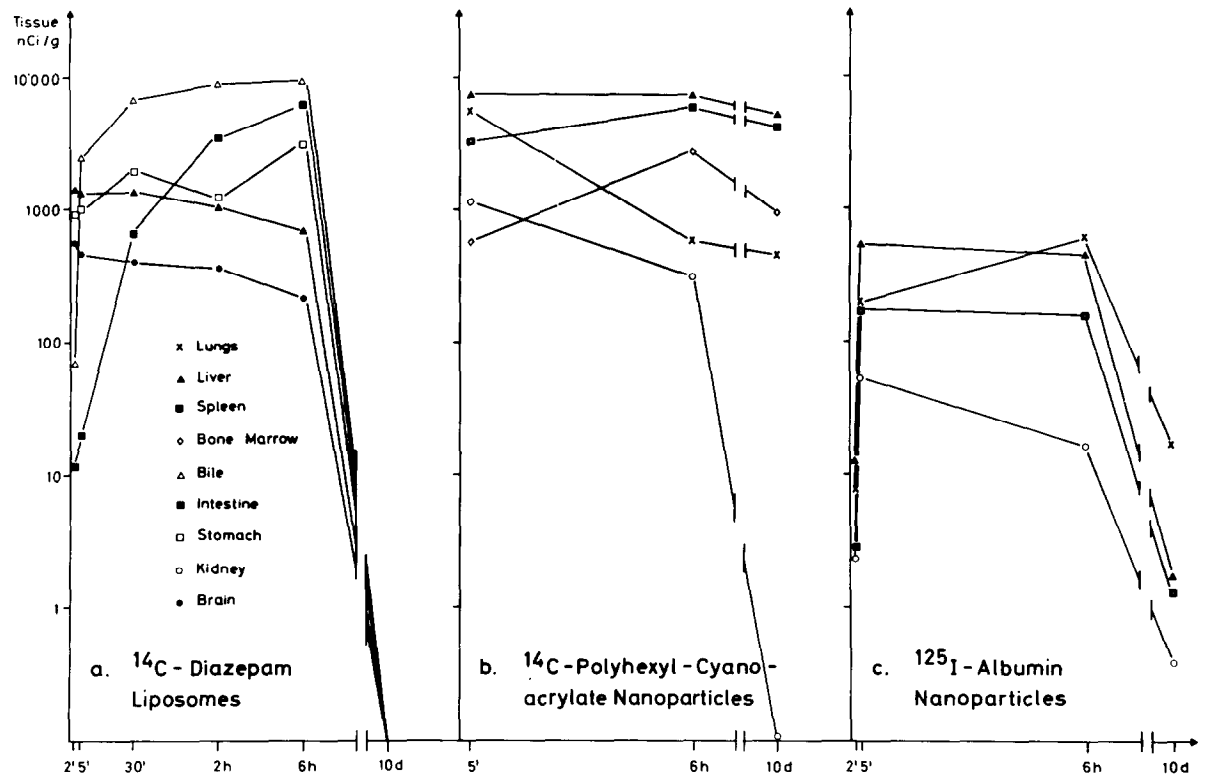

Fig. 9. Distribution of [^{14}C]diazepam liposomes (a), [^{14}C]polyhexylcyanoacrylate nanoparticles (b) and ^{125}I-albumin nanoparticles (c) in the organs with main accumulation after various times up to 10 days following i.v. injection.

Light and electron microscopic distribution and localization of PHCA and albumin nanoparticles inside lungs and liver

Since most of the RA was found in either liver or lungs, only these organ tissues were investigated by light and electron microscopical methods including autoradiography. As we were interested mainly in the fate of the labeled carrier material both types of nanoparticles, PHCA and albumin were examined, whereas the liposome wall materials were not detectable in the tissue.

Light microscopy

Autoradiographs of the lungs of animals sacrificed 5 min after i.v. injection of [^{14}C]PHCA particles show two types of arrangements of silver grains in the tissue. Besides RA dispersed over the whole tissue, aggregated silver grains (clusters) were found in the alveolar epithelium. At this time, single clusters have diameters of 20–30 μm (Fig. 10). In the sinusoidal lumen of the liver tissue the formation of such clusters (arrow in Fig. 11), 5 min after i.v. injection of the particles is less prominent than in the lungs and most of the silver grains were still homogeneously distributed throughout the tissue. 5 min after administration of ^{125}I-albumin particles, light microscopic autoradiographs revealed aggregates of RA with diameters up to 50 μm. Furthermore, multiple aggregates were found with different sizes up to 100 μm. The aggregates were in close association with endothelial cells in the alveoli of the lungs (Fig. 12). Similar aggregates were found in the sinusoidal lumen of the liver, but cluster formation was less prominent than in the lungs, reaching only diameters up to 30 μm (Fig. 13). In both organs, dispersed RA is observed sporadically. The diameters of silver grain-clusters after injection of albumin par-

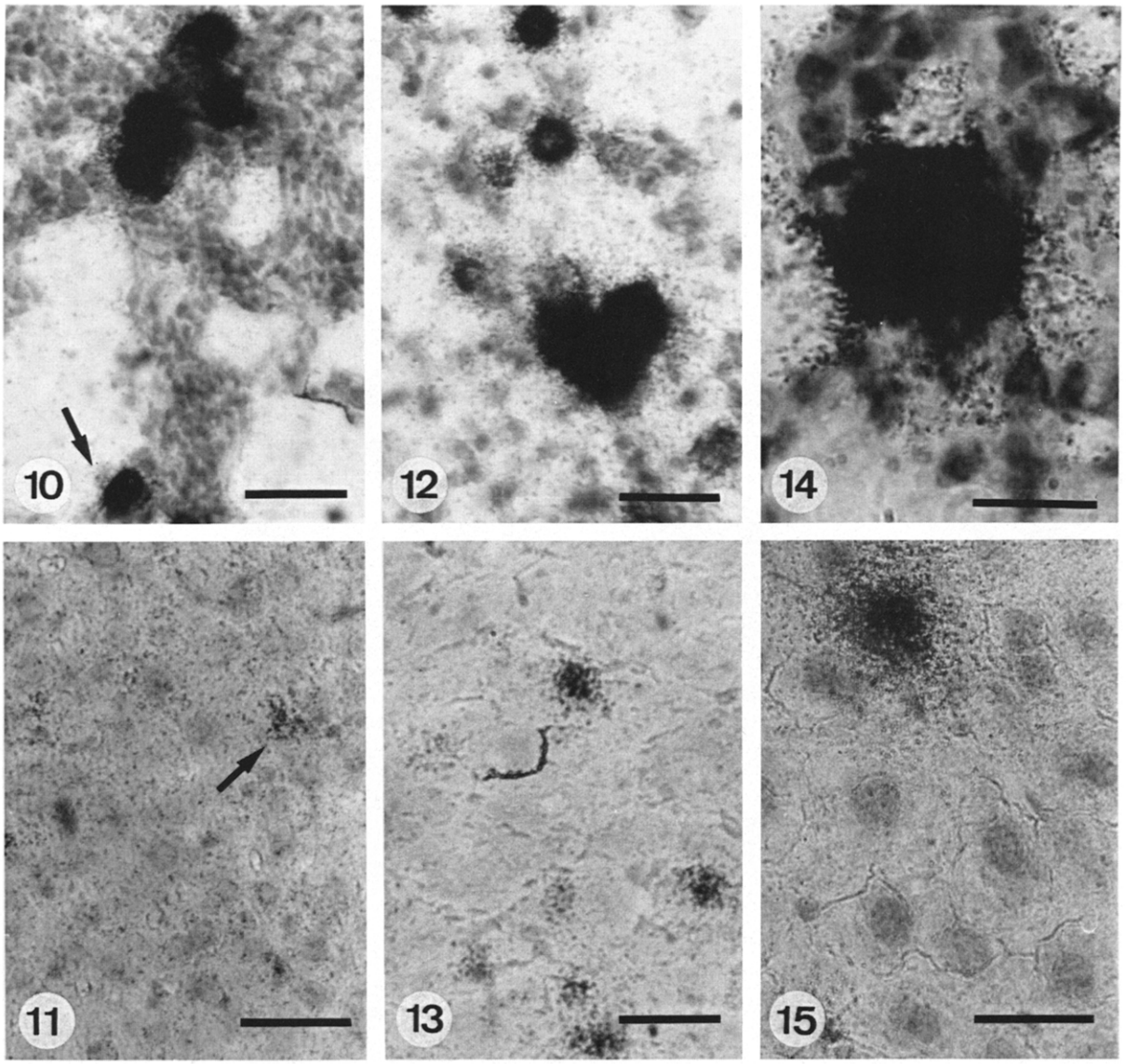

Figs. 10–15.

Fig. 10. Five min after i.v. injection of [^{14}C]polyhexylcyanoacrylate nanoparticles. Dense aggregates of silver grains (radioactivity) are found in the lungs. Discrete radioactivity can also be seen. Bar = 100 μm.

Fig. 11. Five min after i.v. injection of [^{14}C]polyhexylcyanoacrylate nanoparticles. In the liver, radioactivity is detected all over the tissue as discrete dots. Areas with slight accumulation of radioactivity are visible (arrow). Bar = 100 μm.

Fig. 12. Five min after i.v. injection of ^{125}I-albumin nanoparticles. Single and multiple aggregates (clusters) of radioactivity are found in the lungs. Bar = 100 μm.

Fig. 13. Five min after i.v. injection of ^{125}I-albumin nanoparticles. Aggregates of radioactivity are spread over the whole liver tissue. Separate radioactivity is rarely seen. Bar = 100 μm.

Fig. 14. Ten days after i.v. injection of [^{14}C]polyhexylcyanoacrylate nanoparticles. In the lungs, radioactivity is concentrated in multiple aggregates (clusters). Bar = 40 μm.

Fig. 15. Ten days after i.v. injection of [^{14}C]polyhexylcyanoacrylate nanoparticles. In the liver, radioactivity has accumulated in clusters up to 60 μm at the expense of discrete radioactivity. Bar = 40 μm.

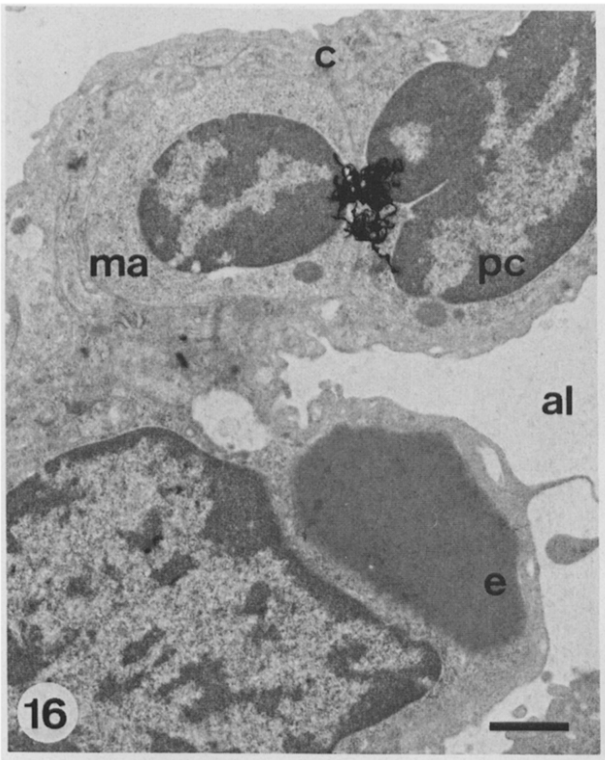
c
ma
pc
al
e
16

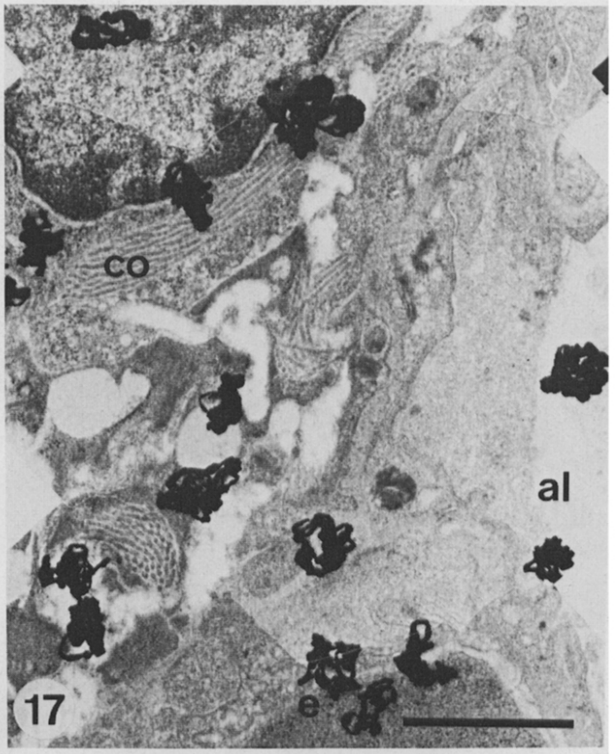
co
al
e
17

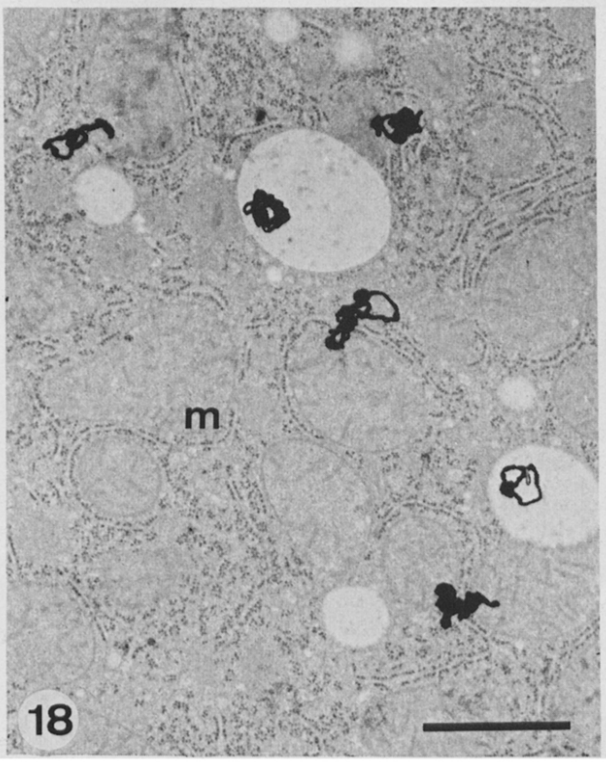
m
18

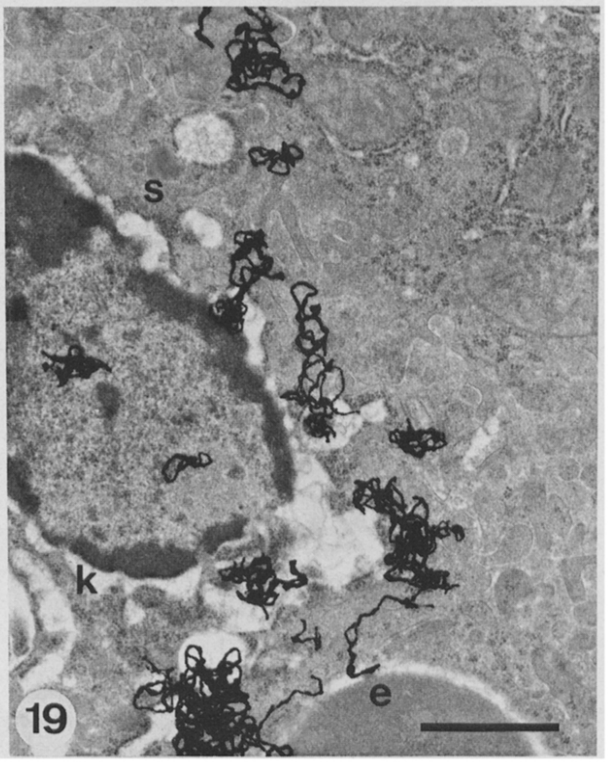
s
k
e
19

ticles decreased with time. Residual aggregates were mainly localized in the periphery of both organs. After 10 days, RA had disappeared.

In contrast to these findings, [^{14}Cs]PHCA particles showed a different distribution pattern of clusters. In the liver and lungs clusters persisted during the observed period of 10 days (Figs. 14 and 15). Furthermore, an increase in the numbers of clusters was observed in both organs, whereas an increase in the size of the clusters was found exclusively in liver.

Electron microscopy

Five min after i.v. injection of [^{14}C]PHCA particles RA of these slow degrading particles was found inside the lung capillaries beside erythrocytes, partly phagocytized by macrophages and already inside endothelial cells and connective tissue (Fig. 16). As individual particles are not recognizable, only aggregates of silver grains were observed. After 6 h, they are dispersed in the endothelial cells of the alveoli and in the connective tissue, and 10 days after the administration, evidence for cluster formation in different cell types such as endothelial cells, macrophages and septal cells of the alveolar sacs appears (Fig. 17). In the liver, RA was detected 5 min after i.v. administration in the capillary system, the sinusoidal lumen, in Kupffer cells and already in hepatocytes (Fig. 18). A few hepatocytes contained silver grains persisting for 10 days. Clusters were formed in all cell types of the sinusoidal lumen (Fig. 19) and the hepatic cells themselves.

^{125}I-albumin particles were localized 5 min after i.v. injection mostly in the capillaries of the lungs (Fig. 20) and phagocytized by macrophages. They showed strong tendency to aggregate and form clusters. The degradation by proteases produced free silver grains inside the tissue (Fig. 21). Even 10 days after administration aggregates were found in capillaries in a decreasing amount.

In the liver, the ^{125}I-albumin particles were found in the sinusoids after 2 and 5 min (Fig. 22) often surrounded by Kupffer cells. The tendency for aggregation was less pronounced than in the lungs. After 6 h, intact particles remained inside the Kupffer cells (Fig. 23) and silver grains from degraded particles were found in the hepatocytes. The picture changed only little within the next 10 days.

Discussion

Kinetics

All 3 preparations, [^{14}C]diazepam liposomes, [^{14}C]PHCA nanoparticles and ^{125}I-albumin nanoparticles showed a similar distribution in the RES of different organs (liver, lungs, spleen and bone marrow). An accumulation in the RES is typical for colloidal particles (Gregoriadis, 1974; Kimelberg et al., 1976; Gregoriadis et al., 1977; Kreuter, 1983b, 1985).

Due to the diazepam label in the lipid layer of liposomes a relatively high level of RA was found in the bile and in the brain in comparison to the two other types of nanoparticles. Nevertheless, the accumulation of diazepam in the brain is much lower when incorporated into liposomes than after administration of free diazepam (Keller and

←

Figs. 16–19. Electron microscopic autoradiographs.

Fig. 16. Five min after i.v. injection of [^{14}C]polyhexylcyanoacrylate nanoparticles. In the lungs, silver grains (radioactivity) are localized in capillary vessels (c), near macrophages (ma) and polymorphonuclear cells (pc).

Fig. 17. Ten days after i.v. injection of [^{14}C]polyhexylcyanoacrylate nanoparticles. In the lungs, radioactivity is typically found in clusters, localized inside all different cell types.

Fig. 18. Five min after i.v. injection of [^{14}C]polyhexylcyanoacrylate nanoparticles. In the liver, radioactivity is incorporated into hepatocytes.

Fig. 19. Ten days after i.v. injection of [^{14}C]polyhexylcyanoacrylate nanoparticles. Radioactivity is found accumulated in clusters near the sinusoidal lumen (s). Bars = 1 μm; c, capillary vessel; e, erythrocyte; k, Kupffer cell; m, mitochondria; s, sinusoidal lumen; al, alveolar lumen; co, collagen fibres.

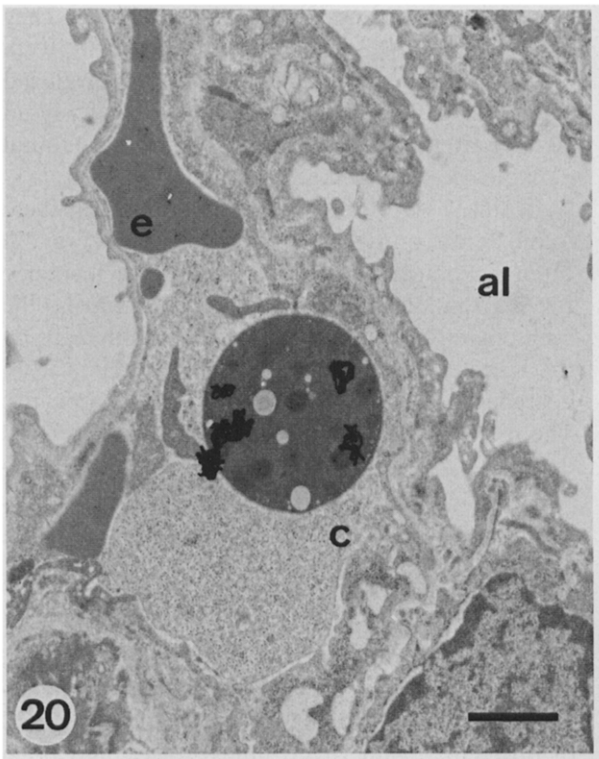
e
al
c
20

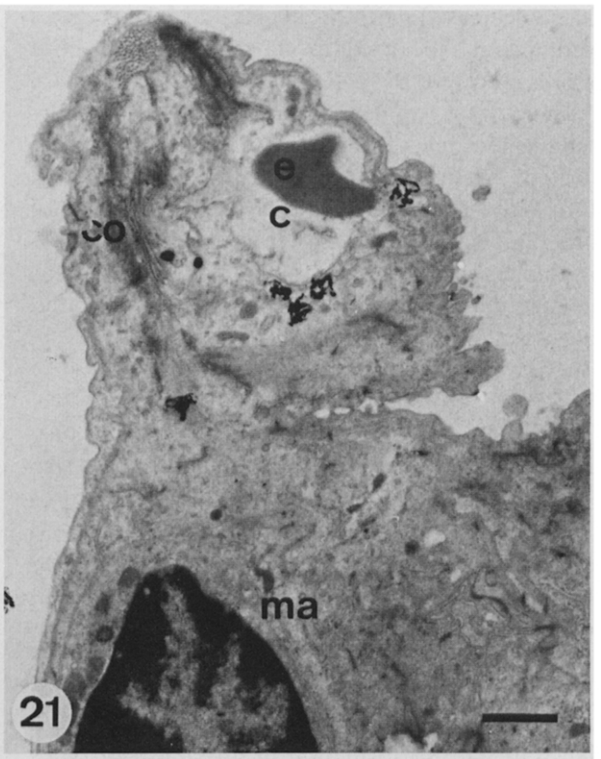
e
c
co
ma
21

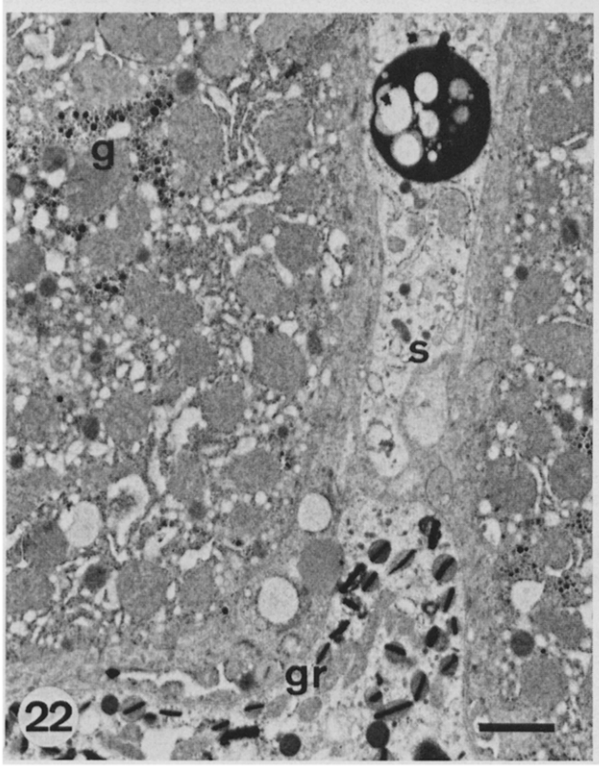
g
s
gr
22

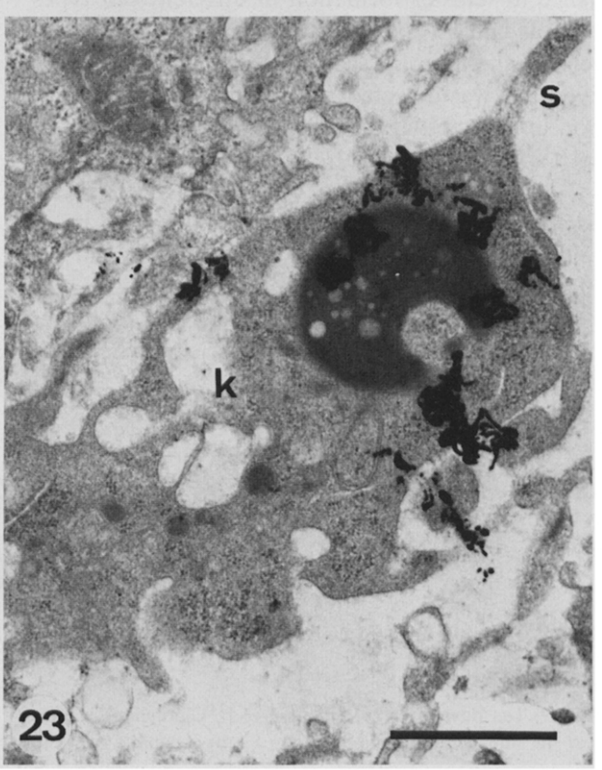
s
k
23

Waser, 1984). Diazepam excreted with the bile into the intestine indicates that it is very tightly bound to the ULL and excreted together with the lipids.

The preparation of uniform albumin nanoparticles was difficult. The iodine label induces the formation of large albumin particles. Furthermore, albumin particles exhibit a strong tendency for aggregation and the reproducibility of particle size was poor in comparison to the other preparations. Although these preparations were filtered prior to drying, aggregates were formed after resuspension despite the use of a detergent (Polysorbate 80) combined with sonication. The centrifuged supernatant fraction of homogeneous particles accumulated to a high degree in the lungs where the first capillary bed after i.v. injection is passed. In the whole body autoradiographs RA in the lungs is always much higher than in other organs (Figs. 3 and 6).

The differences between the kinetics of the 3 carrier systems was especially pronounced after 10 days. The liposome-associated label was totally excreted and the activity of the ^{125}I-albumin particles decreased to the initial activity. In the lungs about 90% decrease of the albumin activity was observed (Fig. 9c). The PHCA particle-associated RA was excreted more slowly. A similar observation was made in nude mice by Gipps et al. (1986), where 45% of the injected dose remained in the liver for 28 days. In contrast, 75% of the initial dose of another cyanoacrylate derivative (polyisobutylcyanoacrylate) was excreted within 24 h (Grislain et al., 1983).

Morphology of liver and lung tissue invaded by nanoparticles

The clearance of injected nanoparticles from the blood stream occurs mainly by Kupffer cells of the liver and by macrophages of the spleen and the lungs and to a lesser extent in the bone marrow. With the electron microscope we can also find RA in the liver sinusoidal compartment and in the hepatocytes as early as 5 min after i.v. injection of PHCA particles (Fig. 18). At this time degradation processes of PHCA contribute to the observed RA only to a negligible amount of 0.1% (Kreuter et al., 1984; Lenaerts et al., 1984). We therefore assume that intact particles were taken up into these cells. Small particles (diameter 100–200 nm) may enter directly through fenestration into the endothelial cells lining the sinusoids (Wisse, 1970; Praaning-van Dalen et al., 1981). The interaction of cells with nanoparticles and possibly other colloids may be different in a living organism than in tissue cultures of hepatocytes (Kreuter et al., 1984). Poste et al. (1982) did not observe uptake of liposomes by parenchymal cells even 4 h after injection.

In contrast to [^{14}C]PHCA particles, ^{125}I-albumin particles were easily detected by their size and their electron-dense appearance in transmission electron microscopy. They showed tendency for aggregation which may lead to emboli in capillaries. Penetration of whole particles into hepatocytes was observed neither at early time (5 min) nor at later times (6 h, 10 days) after injection into the animals. Free RA liberated from the particles was observed inside macrophages and the

←

Figs. 20–23. Electron microscopic autoradiographs.

Fig. 20. Five min after i.v. injection of ^{125}I-albumin nanoparticles. In the lungs, label (radioactivity) and particles coincide and are found inside capillary vessels (c).

Fig. 21. Ten days after i.v. injection of ^{125}I-albumin nanoparticles. In the lungs, radioactivity is found detached from nanoparticles, inside epithelial cells.

Fig. 22. Five min after i.v. injection of ^{125}I-albumin nanoparticles. In the liver, radioactivity bound to the particles, is localized in the sinusoidal lumen (s). Particles are not yet phagocytized by Kupffer cells.

Fig. 23. Six h after i.v. injection of ^{125}I-albumin nanoparticles. In the liver, radioactivity is found together with particles inside Kupffer cells (k) and translocated from the particles as the result of onset of proteolytic degradation. Bar, 1 μm; c, capillary vessel; e, erythrocyte; g, glycogen; al, alveolar lumen; co, collagen; gr, granulocyte; ma, macrophage.

tissue within 6 h and 10 days after injection (Figs. 21, 23). Thus distribution of proteolytic degradation products into extravascular compartments of the lungs and into the hepatic cells may occur by passive transfer from cells of the RES or by transport with the blood into the tissue.

The uptake of particles into the lungs depends on the size and the surface characteristics (Wilkins and Myers, 1966). Five min after administration of ^{14}C-labeled PHCA nanoparticles, autoradiographs revealed adsorption to the surface of macrophages, polymorphonuclear cells, erythrocytes and epithelial cells (Fig. 11) in the lungs and Kupffer cells in the liver. At later times (6 h, 10 days) RA was found in all cell types of the lungs (Fig. 17) and the liver, most probably resulting from degradation products. However, it should be remembered that intact particles were undetectable by electron microscopy. Observations by Adlersberg et al. (1969) showing an increase in lung RA between 24 h and 6 weeks after i.v. injection of slowly degradable polystyrene nanoparticles were interpreted as redistribution of particles previously picked up by other organs of the RES. Poste et al. (1982) also found mononuclear cells containing liposomes 4 h after i.v. administration in the alveolar spaces but never observed transcapillary migration of free liposomes. However, we did not detect macrophages containing labeled material that had left the lung capillaries.

An unexpected spotted appearance of RA was found in whole body autoradiographs (Figs. 3, 5–8) and especially in light microscopic autoradiographs (Figs. 10–15). It is possibly caused by microemboli of both nanoparticle systems, but not by thrombotic accumulation of erythrocytes in small vessels.

Comparative analysis for cluster formation in lungs and liver by light microscopic autoradiography revealed remarkable differences between the two carrier systems. PHCA nanoparticles were first (5 min) found mainly in the form of discrete particles. Within 6 h small dispersed aggregates as well as large dense clusters of RA were found in the tissue at the expense of widely distributed silver grains. Aggregates formed by albumin nanoparticles in capillaries show a maximum size within the first minutes after i.v. administration and diminish gradually in size within the following 10 days due to degradation and deglomeration. Furthermore, neither passage of these large particles through the endothelial layer of the capillaries in the lungs nor phagocytosis of the spheric albumin particles by hepatocytes in the liver seems to be possible. In contrast to the albumin nanoparticles, the growth of clusters of PHCA nanoparticles indicates a slower kinetic mechanism of aggregation.

References

Adlersberg, L., Singer, J.M. and Ende, E., Redistribution and elimination of intravenously injected latex particles in mice. *J. Reticuloendothel. Soc.*, 6 (1969) 536–560.

Couvreur, P., Kante, B., Roland, M., Guiot, P., Baudhuin, P. and Speiser, P.P., Polycyanoacrylate nanocapsules as potential lysosomotropic carriers: preparation, morphological and sorptive properties. *J. Pharm. Pharmacol.*, 31 (1979) 331–332.

Cross, S.A.M., Groves, A.D. and Hesselbo, T., A quantitative method for measuring radioactivity in tissue sectioned for whole body autoradiography. *Int. J. Appl. Radiation Isot.*, 25 (1974) 381–386.

Gallo, J.M., Hung, C.T. and Perrier, D.G., Analysis of albumin microsphere preparation. *Int. J. Pharm.*, 22 (1984) 63–74.

Gipps, E.M., Arshady, R., Kreuter, J., Groscurth, P. and Speiser, P.P., Distribution of polyhexyl cyanoacrylate nanoparticles in nude mice bearing human osteosarcoma. *J. Pharm. Sci.*, 75 (1986) 256–258.

Gregoriadis, G., Structural requirement for the specific uptake of macromolecules and liposomes by target tissue. In J.M. Tager, G.J.M. Hooghwinkel and W.T. Daems (Eds.), *Enzyme Therapy of Lysosomal Storage Diseases*, North-Holland, Amsterdam, 1974, pp. 131–148.

Gregoriadis, G., Neerunjun, D.E. and Hunt, R., Fate of liposome-associated agent injected into normal and tumor-bearing rodents. Attempts to improve localization in tumor tissues. *Life Sci.*, 21 (1977) 357–370.

Gregoriadis, G. (Ed.) *Drug Carriers in Biology and Medicine*, Academic, London, 1979.

Grislain, L., Couvreur, P., Lenaerts, V., Roland, M., Deprez-Decampeneere, D. and Speiser, P.P., Pharmacokinetics and distribution of a biodegradable drug-carrier. *Int. J. Pharm.*, 15 (1983) 335–345.

Juliano, R.L. (Ed.), *Drug Delivery Systems. Characteristics and Biomedical Applications.* Oxford University Press, New York, 1980.

Kanke, M., Simmons, G.H., Weiss, D.L., Bivins, B.A. and DeLuca, P.P., Clearance of ^{141}Ce-labeled microspheres from blood and distribution in specific organs following intravenous and intraarterial administration in Beagle dog. *J. Pharm. Sci.*, 69 (1980) 755–762.

Keller, F. and Waser, P.G., Brain pharmacokinetics of centrally acting drugs. A quantitative autoradiographic study. *Arch. Int. Pharmacodyn.*, 167 (1984) 200–211.

Kimelberg, H.K., Tracy, T.F., Biddlecome, S.M. and Bourke, R.S., The effect of entrapment in liposomes in the in vivo distribution of ^{3}H-methotrexate in a primate. *Canc. Res.*, 36 (1976) 2949–2957.

Kreuter, J., Evaluation of nanoparticles as drug-delivery systems. I. Preparation methods. *Pharm. Acta Helv.*, 58 (1983a) 196–209.

Kreuter, J., Evaluation of nanoparticles as drug-delivery systems. II. Comparison of the body distribution of nanoparticles with the body distribution of microspheres (diameters >1 μm), liposomes and emulsions. *Pharm. Acta Helv.*, 58 (1983b) 217–226.

Kreuter, J., Wilson, C.G., Fry, J.R., Paterson, P. and Radcliff, J.H., Toxicity and association of polycyanoacrylate nanoparticles with hepatocytes. *J. Microencapsul.*, 1 (1984) 253–275.

Kreuter, J., Factors influencing the body distribution of polyacrylic nanoparticles. In P.A. Buri and A. Gumma (Eds.), *Drug Targeting*, Elsevier, Amsterdam, 1985, pp. 51–63.

Lenaerts, V., Nagelkerke, J.F., Van Berkel., T.O.C., Couvreur, P., Grislain, L., Roland, M. and Speiser, P.P., In vivo uptake and cellular distribution of biodegradable polymetric nanoparticles. In D.L. Knook and E. Wisse (Eds.), *Sinusoidal Liver Cells*. Elsevier, Amsterdam, 1982, pp. 343–352.

Lenaerts, V., Couvreur, P., Christiaens-Leyh, D., Joiris, E., Roland, M., Rollman, B. and Speiser, P., Degradation of poly(isobutylcyanoacrylate)nanoparticles. *Biomaterials*, 5 (1984) 65–68.

Leu, D. Manthey, B., Kreuter, J., Speiser, P.P. and DeLuca, P.P., Distribution and elimination of coated poly[2-^{14}C]methacrylate nanoparticles after intravenous in rats, *J. Pharm. Sci.*, 73 (1984) 1433–1437.

Müller, M., Marti, Th. and Kriz, S., Improved structural preservation by freeze substitution. In Brederoo, T. and de Priester, W. (Eds.), *Proc. 7th Europ. Congr. Electron Microsc., The Hague, Vol. 2,* Europ Congr. on Electron Microsc. Foundation, Leiden, The Netherlands, 1980, pp. 720–721.

Müller, U., Munz, K. and Waser, P.G., Incorporation of small unilamellar liposomes loaded with horseradish peroxidase into isolated nerve endings from electric organ of *Torpedo marmorata. J. Neurocytol.*, 12 (1983) 507–516.

Poste, G., Bucana, C., Raz, A., Bugelski, P., Kirsh, R. and Fidler, I.J., Analysis of the fate of systemically administrated liposomes and implications for their use in drug delivery. *Cancer*, 4 (1982) 1412–1414.

Praaning-van Dalen, D.P., Brouwer, A. and Knook, D.L., Clearance capacity of rat liver Kupffer, endothelial and parenchymal cells. *Gastroenterology*, 81 (1981) 1036–1044.

Rogers, A.W., Autoradiography with the electron microscope. In *Techniques of Autoradiography* 3rd edn., Elsevier, Amsterdam, 1979, pp. 387–413.

Scheffel, U., Rhodes, B.A., Natarjan, T.K. and Wagner Jr. H.N., Albumin microspheres for studies of the reticuloendothelial system. *J. Nucl. Med.*, 13 (1972) 498–503.

Slack, J.D., Kanke, M., Simmons, G.H. and DeLuca, P.P., Acute hemodynamic effects and blood pool kinetics of polystyrene microspheres following intravenous administration, *J. Pharm. Sci.*, 70 (1981) 660–664.

Widder, K.J., Flouret, G. and Senyei, A., Magnetic microspheres: Synthesis of a novel parenteral drug carrier. *J. Pharm. Sci.*, 68 (1979) 79–82.

Wilkins, D.J. and Myers, P.A., Studies on the relationship between the electrophoretic properties of colloids and their blood clearance and organ distribution in the rat. *Brit. J. Exp. Pathol.*, 47 (1966) 568–576.

Wisse, E., An electron microscopic study of the fenestrated endothelial lining of rat liver sinusoids. *J. Ultrastruc. Res.*, 31 (1970) 125–150.